CORPUS PUBLISHERS

Journal of Mineral and Material Science (JMMS)

Volume 1 Issue 4, 2020

Article Information

Received date :October 20, 2020

Published date: November 26, 2020

*Corresponding author

Joshi Gaurang R, Assistant professor, Mechanical Engineering Dept, Marwadi University, Rajkot, Gujarat, India

Keywords

Friction Stir Welding; Additional Heating & Cooling; Dissimilar Metal Joining; Butt Joint; Gas Tungsten Arc Welding Torch

Research Article

Evaluating the Tensile Fracture Mechanism of Friction Stir Welded Cu to SS Material

Joshi Gaurang R[1]*, Vishvesh J Badheka[2]

[1]Assistant professor, Mechanical Engineering Dept, Marwadi University, Rajkot, Gujarat, India

[2]Professor, Mechanical Engineering Dept, School of Technology, PDPU, Gandhinagar, Gujarat, India

Abstract

The analysis of tensile fracture pattern in correlation with the welding parameters and metallurgical test results enlighten in service weld quality of material being welded. Modern industry is seeking to establish optimum method which can incorporate multiple properties within single structural component; welding is one of the way to do so. Hence, dissimilar material welding is exploited in recent years. Friction stir welding (FSW) is a solid state, hot-shear process. It can eliminate or reduce detrimental problems associated with melting (in fusion welding processes) of materials such as porosity, solidification cracking, and residual stress. These issues may trigger premature failure of the joint. Cu with SS welded joints are suitable enough to construct first wall and divertor; structural components of international thermo-nuclear experimental reactor. This is the reason of present study focuses on to friction stir welding of Cu with SS aiming to improve mechanical properties. It can be achieved by optimal combination of welding parameters. Dissimilar metal joining through friction stir welding process has been adequately evaluated in recent past. However, limited research work has been reported in present system. Hence, a fully experimental approach has been adopted in the present investigation to exploit the effect of assisted source on to joint formation.

A gas tungsten arc welding torch in the range of 20A to 60A with an interval of 20A is applied at the leading side of the friction stir welding tool on joint line as assisted heating source. Furthermore, 15 psi as well as 30 psi of compressed air and 75 ml/min of water cooling is applied at the trailing edge of joint as assisted cooling while transverse phase of process. In conjunction with theses welding parameters, authors are aiming to investigate tensile fracture mechanism on the scale of micro-hardness and metallurgical test results. Tensile test result is reported that the joint efficiency vary from 58% to 72% when material welded with assisted heating whereas 75% in the case of normal mode of friction stir welding. However, there was a steep drop in the joint efficiency when forced air/ water cooling of joint was employed during the process. The joint efficiency was only 29% with water cooling whereas slight improvement observed (43%) when material welded with compressed air cooling. Maximum hardness in the weld nugget is obtained for conventional FSW samples. Most of the samples tested for mechanical strength fractured in the nugget area. Some of them fractured from the interface of Cu/SS or suspended SS particles (present at weld nugget) Reported poor strength. Most of the welded samples wear fractured from Cu/SS interface during additional cooling while friction stir welding. Higher tensile strength and ductile fracture behavior are observed in joints fabricated with additional heating as compared to additional cooling. This indicates improved dynamic deformation resulting due to better material flow within the joint for heating assisted FSW joints as compared to force cooled joints.

Introduction

The fusion reactor is one of the few eco-friendly methods available to produce energy. Its integral structures absorb a large quantity of accelerated particles while power generation. Though, it causes energy transformation from the accelerated particles to the wall. Eventually, the blanket system of the first wall is exposed to elevated temperature [1]. Thus, temperature control within the structure is a major concern for the duration of the fusion process. The international thermonuclear experimental reactor (ITER) has been built to establish sustainable fusion energy resource [2]. In order to operate these structures at elevated temperature, rapid dissipation of heat is necessitated. However, material having higher thermal conductivity is suitable as structural component i.e. Copper (Cu). At the other hand, structure demand high strength at elevated temperature to absorb the impact of accelerated particle i.e. Stainless Steel (SS). In this context, Cu bonded with austenitic SS could meet the said requirement. Dissimilar metal joining such as Cu to SS is a challenging task looking towards its diversified properties across the faying surfaces like difference in coefficient of thermal expansion, thermal conductivity, dilution, melting points and solubility. Even though, Cu to SS can be welded successfully using fusion and non-fusion welding processes [3-10]. Fusion welding of dissimilar material faces problems related to porosity, solidification cracking, residual stress, difference in thermal conductivity and micro-segregation i.e. due to different melting points. Laser Beam Welding (LBW) and Electron Beam Welding (EBW) of both material have revealed adequate results. However, these processes are expensive, and it requires high degree of control over process which make them complex. Explosive welding has reported excellent weld quality. In contrast, there is a limitation on the part geometry of the material being welded. Furthermore, controlled explosions are expensive, risky and requires very high skill levels. Due to these aspects, Friction Stir Welding (FSW) is being largely investigated for use for dissimilar metal joining [11, 12].

Friction Stir Welding Technology (FSWT) is a solid-state welding technique that was invented at the welding Institute (TWI, Abington, Cambridge, UK) [13]. It is a solid state, hot shear process [13-16] in which non-consumable rotating tool with shoulder and pin is inserted into abutting surface till the shoulder rub against work-piece. The tool is then transverse along abutting surfaces of the plates. FSW of dissimilar metal involves unique set of challenges [11, 17] like different deformation behavior of material, physical properties i.e. thermal conductivity across the faying surfaces. Moreover, it faces problems related to reliability of tool, solubility of material and formation of detrimental intermetallic compounds. These factors and others contribute to the asymmetry in both heat generation and material flow. Previously reported literature exposed the fact that FSW has potential to joint dissimilar material, even in cases where materials are considered un-weldable by conventional welding processes such as Al-Steel, Al-SS [18-22]. However, FSW of Cu and SS is relatively less researched [23, 24]. It was reported that sound FSW of Cu to SS can be achieved by placing SS (Higher melting point) at advancing side and Cu (Lower melting point) at retreating side. This is due to the higher specific energy (higher torque) leading to higher heat input at advancing side compare

to retreating side [25]. It was reported that FSW of Cu to SS can be achieved by offsetting the tool towards retreating side [23, 24]. This reduces the load on the tool and prevents the formation of detrimental intermetallic compound within the joint resulting in improved strength of the joint.

In the present investigation, high thermal conductivity of Cu and low of SS raise the issue of heat balance. Hence, authors have suggested applying an additional source of the heating [26] and cooling [27] during FSW. This process is termed as hybrid or assisted FSW. A GTAW torch is applied at the center line of the joint, ahead of the tool which pre heats the Cu. Preheating reduces the cooling rate of the joint & may provide enhanced material flow within the joint area. It also decreases the heterogeneity of deformation across the faying surface. Furthermore, additional cooling reduces the excessive grain growth resulting due to continuous dynamic recrystallization. A sound joint is subject to parametric control over the process. Therefore, this study is aiming to investigate the parametric effect of the process on the tensile properties of the joint.

Material & Methods

Experimental work has been undertaken at The Advanced Welding Research Laboratory, at the Mechanical Engineering Department, Pandit Deendayal Petroleum University (PDPU), India. FSW experiments of 3 mm thick Cu to SS were conducted at constant parameters; feed rate of 31.5 mm/min, 1500 RPM, 2° tilt angle and 2 mm tool pin offset under both additional cooling and heating mode of FSW to evaluate the effect of assisted heating on Cu to SS joint formation. Additional details of parameters used for weld trials is as shown below.

a. Additional cooling: - A Compressed air of 15 psi and 30 psi was employed at the trailing side of tool during a process. Water cooling was also undertaken at a rate of 75 ml/min.
b. Additional heating: - A GTAW torch was applied as separate trials at the leading side of FSW tool at Cu side, 2 mm away from butt line (at a joint line). GTAW parameters; 20,40,60 amperage, 2.4 mm electrode diameter, straight polarity, direct current power source, 20 volts, 45° electrode angle, torch angle is of 45° with respect to a spindle head [26].
c. Pilot Hole Dimensions: 3 mm diameter and depth is of 1.5 mm [28].

Results and Discussion

a) Macrostructure

The observed macrostructure (Figure 1) of welded specimen during conventional FSW, heat assisted FSW and welds with forced cooling reveal dispersed SS particle into Cu metal matrix. Location and the size of particle largely vary with the combination of parameters used in trials. Larger mixing of SS in Cu metal matrix were observed within the joint during FSW with additional heating and conventional FSW as compared to welds with additional cooling. This indicates relatively poor material flow in the case of material welded with forced cooling than other welded samples.

Macrographs also indicate reduced mixing of the two material in the joint area as the pre-heating current is increased and with increase in additional cooling. The highest amount of mixing of material in the nugget area for heat assisted FSW was achieved during trials with the 20A pre-heating current.

The macrographs shows clear indication of continuous dynamic deformation. Frictional heating of the tool alter the macro and microstructure. It is influenced by thermal properties of the Cu and SS and also by rotational and transverse speed of the tool. Material flow for weld trials with forced cooling is restricted due to rapid dissipation of heat from the weld area. The mixing of the SS and Cu particles within the nugget area is limited during these trials and the SS particles are generally found at the root area of the joint. The rotation and forward motion of the tool causes increased local stresses that exceed critical flow stress and resulting in plastic deformation. This deformation forces material to flow within the joint. The level of deformation depends on the availability of heat in the joint area which is higher for the heat assisted and the conventional FSW and hence, the largest deformation and mixing of the two material with the weld nugget is achieved for these two conditions. This improved mixing provides weld joints with higher tensile strength. The macrographs concludes that tensile strength improves if amount of SS dispersed particle increases within the weld nugget (WN).

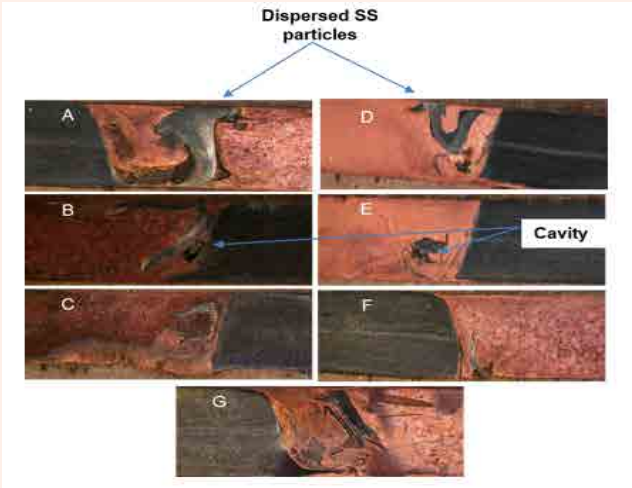

Figure 1: Macrographs of welded sample at (A) 20A (B) 40A (C) 60A additional heating, (D) 15 psi (E) 30 psi compressed air cooling, (F) 75 ml/min water cooling & (G) Normal FSW.

b) Microstructure

FSW of dissimilar metal welding is difficult to achieve, especially for materials having low solubility like Cu and SS. In order to achieve joints with better metallurgical characteristics, the WN should be a composite metal matrix of both the metals being welded. The microstructure (Figures 2-4) of the joint has been examine across the welded plate area and base metal (BM). Uniform distribution of grains is seen through micrograph of both BM. Large grains are observed in the case of Cu BM compared to SS BM. The microstructure evolution of the welded joint depends on the chemical composition of materials and parametric condition of process such as heating rate, cooling rate, mechanical loading. The microstructure of weld joints are shown when material welded at 20A pre-heating current in (Figure 2), normal mode of FSW in (Figure 3) and 30 psi forced cooling in (Figure 4). The study clearly reveals distinct zones like BM, heat-affected zone (HAZ), thermo-mechanical affected zone (TMAZ) & WN. Cu BM has a coarse grain structure. Further coarsening has been reported within HAZ and TMAZ than BM when material welded with normal and pre-heating mode of FSW. Elongated grains are observed in the TMAZ as compared to HAZ which may be the result of severe plastic deformation and heat generation. On the other hand, similar HAZ and TMAZ has been observed when material welded with forced cooling which may be the reason of poor strength. In addition to that, WN of all welded sample indicating significant refinement of grains. It is due to continuous dynamic deformation imposed by tool pin on to the joint area.

In the case of additional heating, WN experiences the slip and slick around the tool pin surface while FSW. It is due to high degree of deformation at the center of WN. The microstructure of FSW joints welded at additional heating reveals un-recrystallized band and elongated grains within the WN as compared to normal FSW. These cause a slight decrease in tensile strength for FSW joints when material welded at additional heating. A clear boundary is also observed between two metals in all the joints. The dark zone within the WN represent ultra-fine grains formed due to dynamic recrystallization and is not a cavity [29]. Un-recrystallized elongated grains are observed at TMAZ of SS in all the welded samples reflects lack of plastic deformation resulting due to taper tool pin profile. Tool pin offset and tool geometry indicate minimum contact between tool pin and the SS. When material is welded with additional cooling, poor material flow is observed as most of the dispersed SS particles are suspended and trapped within root side of WN. Lower heat input results in almost similar HAZ and TMAZ at both sides and also increases the probability of defect occurring. Stretched un-recrystallized grains represent brittleness resulting in poor joint strength and metallurgical bonding. There is asymmetry in the microstructure of the weld nugget due to the different deformational behavior experienced by advancing and retreating side of the nugget thereby causing different recrystallization and grain growth behavior within the two areas.

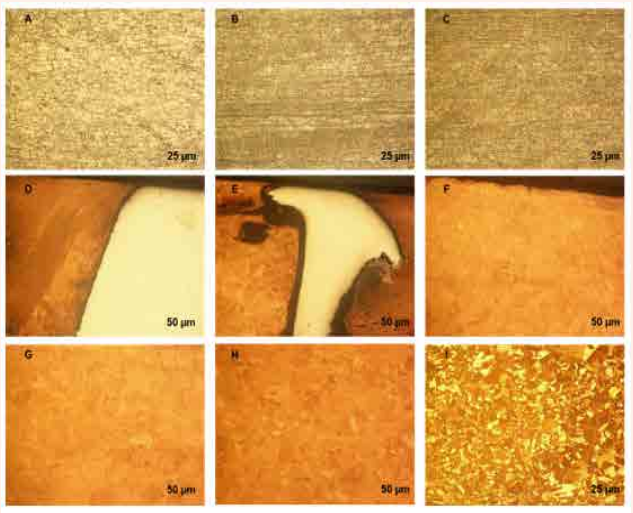

Figure 2: Micrograph of material welded samples at 20A pre-heating current (A) SS BM (B) SS TMAZ (C) SS HAZ (D) Cu/SS interface (E) WN center (F) WN Cu side (G) Cu TMAZ (H) Cu HAZ (I) Cu BM.

c) Micro-hardness

The Micro-hardness profile of the weld is shown in (Figure 5).The distance marked along the X axis is taken from the weld center and zero corresponds to the joint line. Distance between two indentations is 1 mm whereas negative sign corresponds to Cu side and positive corresponds to SS side. Micro-hardness values significantly increases from retreating side to advancing side as both base material has different mechanical properties. Hardness value depends on grain size, smaller grain size of WN area plays an important role to provide better weld strength. This is governed by Hall-petch equation [30]. Maximum hardness corresponding to weld nugget (WN) area as it undergoes large dynamic deformation due to intense stirring. Higher hardness is observed within WN in the case of conventional FSW which may be attributed to a finer grain structure whereas lower hardness at WN when material welded with forced cooling indicating coarsening of the grains. The small particles of inter-metallic compounds also benefit higher hardness according to Orowan mechanism [30]. In contrasts large, suspended particle of SS within WN is the reason of sudden increase in hardness value. At the joint line lowest hardness is reported when material welded with additional cooling. The maximum hardness is obtained in the case of normal mode of FSW. For welds with 30 psi additional cooling, the SS particles are found accumulated very near to the interface making interface (Figure 1) area hard compare to WN which probably is the site of fracture initiation.

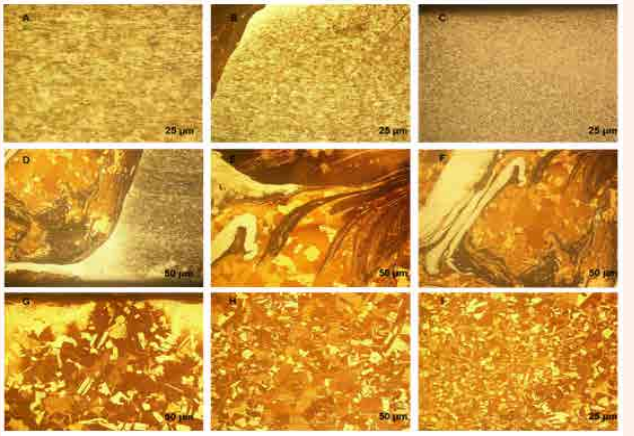

Figure 3: Micrograph of material welded sample at normal FSW (A) SS BM (B) SS TMAZ (C) SS HAZ (D) Cu/SS interface (E) WN center (F) WN Cu side (G) Cu TMAZ (H) Cu HAZ (I) Cu BM.

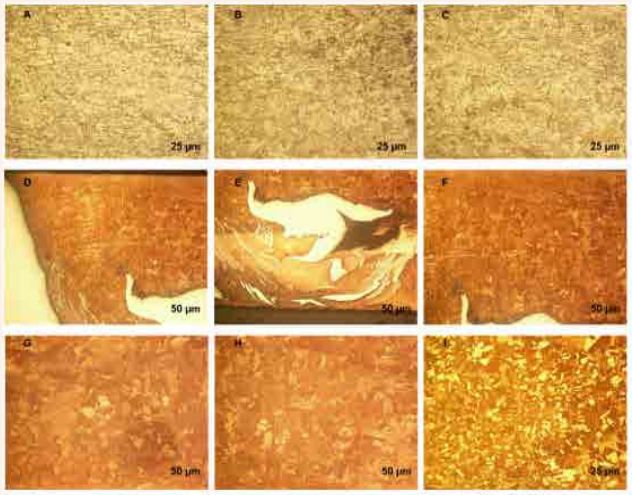

Figure 4: Micrograph of material welded sample at 30 psi additional air cooling (A) SS BM (B) SS TMAZ (C) SS HAZ (D) Cu/SS interface (E) WN center (F) WN Cu side (G) Cu TMAZ (H) Cu HAZ (I) Cu BM.

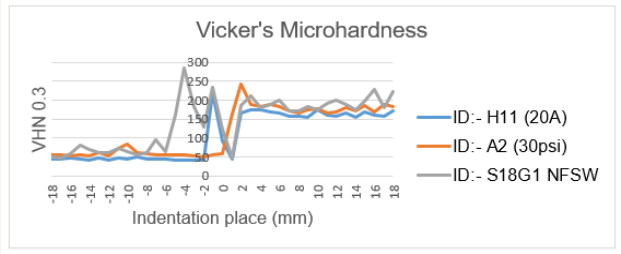

Figure 5: Micro-hardness value of welded samples.

d) Tensile Properties

After welding, tensile specimens (Figure 6) were prepared transverse to the weld direction by electro-discharge machining process (EDM). Tensile test (Table 1) has been carried out at Electrical Research & Development Association (ERDA), India to measure the TS, Joint Efficiency (JE) and elongation of the weld specimens. The tests were conducted as per American Society for Testing Material (ASTM) standard E8M-09 (Figure 6); Cross head speed was maintained at rate of 1.5 mm/min and machine load capacity was 100 KN. The reported TS is the average of five specimen values. It is observed that Joint efficiency (JE) varies from 58% to 73% for FSW joints with additional heating whereas it varies from 29% to 43% for welds with additional cooling. The relatively low efficiency obtained may be attributed to the softening of weld region during FSW. The tensile strength decreases as the pre-heating increases. There is a slight degradation reported in strength of heat assisted FSW over conventional FSW.

Most of the tensile sample were fractured from WN while some of them failed from SS TMAZ near to the interface and SS suspended particle within WN (Figure 7). The welds that failed at the weld nugget displayed higher tensile strength than those that failed at the SS TMAZ (Figure 8). Sample failed from SS TMAZ (Figure 9) corresponds to poor material joining due to heterogeneous deformation mechanism across the faying surfaces. This is due to diversified properties of both material and taper tool design. Minimum contact achieved with SS at root region attributed to taper geometry of tool land up with poor deformation criteria, especially at root side. It decreases the TS value of root region, making them softer compare to top side. Sample fractured from dispersed SS particle (Figure 9) experienced failure due to hardness difference. Suspended particle may stretch due to torque generated by FSW tool rather than the plastic deformation; ideally. This is attributed to higher hardness region within or around the dispersed particle make brittle joint.

Table 1: Tensile properties of welded samples.

Assisted Source	TS (Mpa)	JE (%)	% Elongation
Assisted Heating			
20A	164.88	72.63	9.18
40A	132.5	58.38	4.06
60A	158.36	69.76	11.92
Normal Mode of FSW			
NFSW	173.05	76.23	8.22
Forced Air Cooling			
15 psi	97.72	43.05	7.9
30 psi	99.12	43.67	7.68
Water Cooling			
75 ml/min	66.63	29.35	4.17

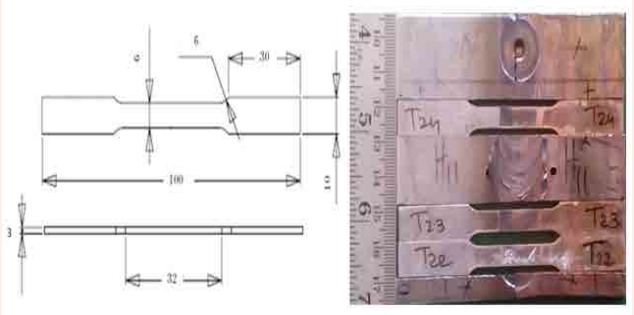

Figure 6: Tensile test specimen as per ASTM E8M-09.

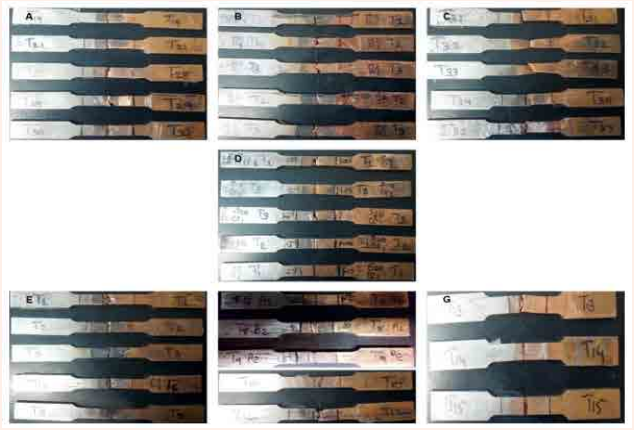

Figure 7: Tensile fracture location photographs of welded sample at (A) 20A (B) 40A (C) 60A pre-heating current, (D) at Normal FSW & (E) 15 psi (F) 30 psi (G) 75 ml/min additional forced cooling.

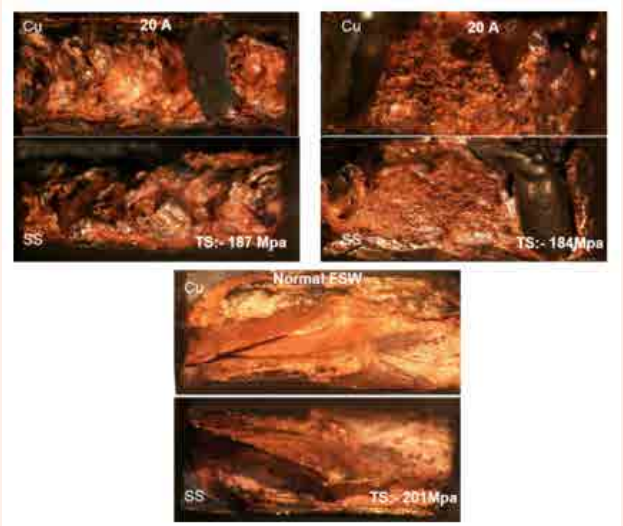

Figure 8: Fracture surface photographs of tensile sample fractured from WN.

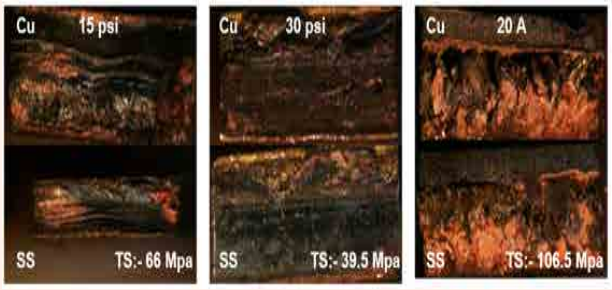

Figure 9: Fracture surface photographs of tensile sample fractured from (left to right – SS suspended particle, SS TMAZ/Interface, SS TMAZ/Interface.

Additional heating soften the material leading to excessive material flow resulting in material expulsion at the edge of shoulder i.e. flash. Amount of flash (Figure 10) is increases as the pre-heating current increases which may be a reason for the reduced TS of these joints when compared to the conventional welds. A higher amount of flash is observed during the FSW with forced cooling as compared to FSW with heating. Poor material flow within the joint area due to inadequate plasticization could be attributed as the reason for the excessive flash. The higher flash is the main cause for reduced tensile strength of these joints when compared to the conventional FSW. The weld joints with 40A pre-heating current indicates presence of a void within the WN (Figure 1) which is the major reason for low tensile strength. Resistance to dislocation is higher at the void location, and they form fracture initiation site under tensile loading which reduces TS value. This large void is a reason of chaotic flow [31]. Metal flow is in opposite direction at below and above the void location leading to vortex generation.

e) Tensile Fracture

An investigation of the tensile fracture does provide insight into the effect of weld parameters on the fracture mechanism in co-relation with metallurgical properties such as microstructure and micro-hardness. Tensile fracture surfaces revealed a significant variation in both the macroscopic morphology and microscopic mechanisms for the welded samples. Scanning Electron Micrographs (SEM) has been carried out to evaluate the fracture behavior. Overall morphology (Figure 11a) was significantly brittle indicating failure from the interface when material welded with forced cooling.

Figure 10: Friction stir welded samples at (A) 20A (B) 40A (C) 60A additional heating, (D) 15 psi (E) 30 psi forced cooling and at (F) 75 ml/min water cooling.

It also represent poor dynamic deformation behavior of material. Further, no traces of dense Cu particle concentration were found on the fracture surface indicating effect of the rapid dissipation of heat. At the other hand, Cu tensile fracture surface (Figure 11b) indicates presence of a hard phase at root side. It indicates that a weak joint is formed at the interface region of Cu. The region was covered by dense distribution of micro and macroscopic voids (Figure 11c).There was also a region that displayed collapsed metal bond where material experiences transition from ductile to brittle fracture. These may be the reasons for the poor TS of joints welded by FSW with external forced cooling. SEM of root fracture surface shows evidence of crack propagation leading to failure (Figure 11d), coalescence of macroscopic voids enhances the chance of fracture. Overall morphology of material welded at pre-heating current (Figure 12A & 12B) suggest large deformation under tensile loading. At the same time, elongated deep hole indicate strong bonding between two materials although, root side of the fracture surface reveals that the failure must have initiated from the root side. The ductile fracture mode is the dominant phenomena observed during the uniaxial tensile loading of the welded coupons (Figure 12C).It can be explained by the void coalescence mechanism and the broken fibrous surfaces (Figure 12D). It also represent the distinct deformation of tensile specimen. At the other hand, dimpled fracture mechanism was investigated along with deep holes. These deep holes corresponding to detached suspended SS or oxide particle (Figure 12C). It also contains small size equiaxed dimples which are distributed uniformly on to the surface. These factors reflect the reasons for the higher joint strength of heat assisted weld over forced cooling FSW. It is due to better recrystallization in the joint area. (Figure 13) shows that TS sample indicating high resistance against the stain deformation concentration at the property damping zone at WN. It also shows the high density of deep hole within the stir zone reflecting insertion of SS suspended particle while process which is the reason of slight increase in the TS value compare to the material welded at 20 A pre-heating current.

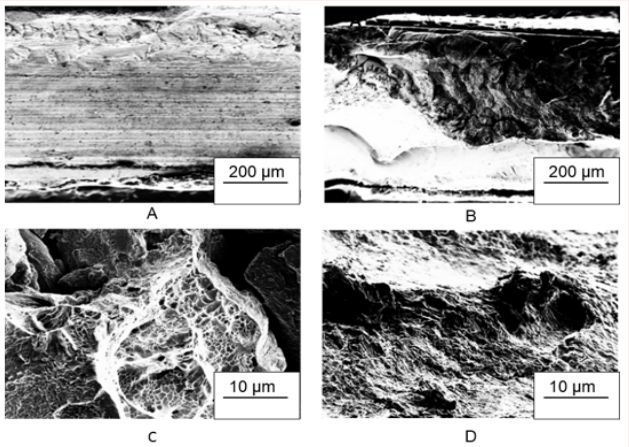

Figure 11: SEM of tensile fracture when material welded with 30 psi additional compressed air, overall morphology of (A) SS side (B) Cu side fractured surface, tensile fractured surface of (C) Centre (D) root of Cu side.

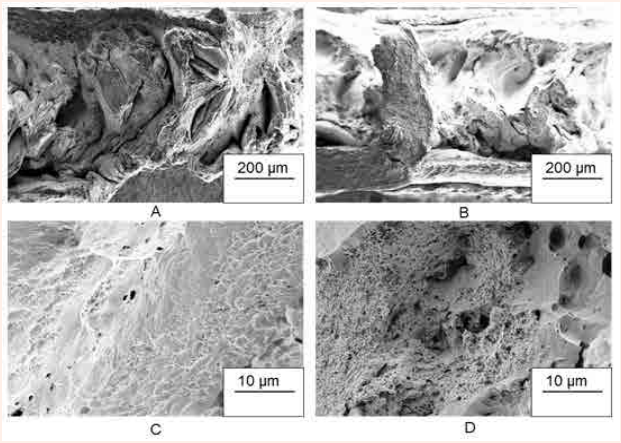

Figure 12: SEM of tensile fracture when material welded with 20A pre-heating current, overall morphology of (A) SS side (B) Cu side fractured surface, tensile fractured surface of (C) Centre (D) top portion of Cu side.

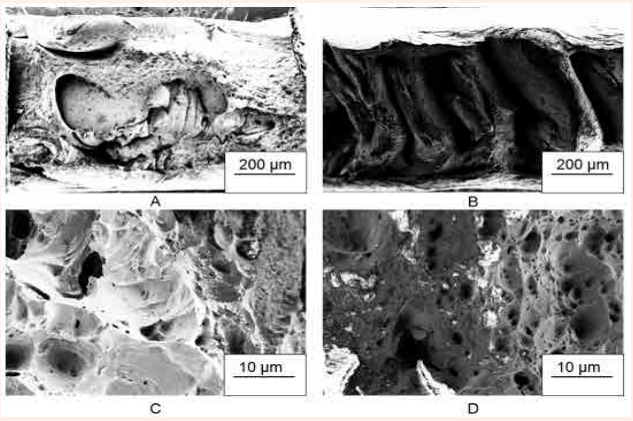

Figure 13: SEM of tensile fracture when material welded with 20A pre-heating current, overall morphology of (A) SS side (B) Cu side fractured surface, tensile fractured surface (C) Centre of SS side and (D) Centre of Cu side.

f) Fracture Mechanism

The Inhomogeneity in deformation while straining of tensile specimen in the uniaxial direction is due to diverse property field across the faying surface and shearing of strengthening precipitate dispersed through the metal matrix. These kind of inhomogeneity in deformation is concentrated in the area of microstructure where large SS suspended particle or high dense SS region within the nugget are found. It promote brittleness locally. This feature can further conduct the macroscopic voids. These macroscopic voids form a dimple due to continuous growth under deformation. Voids transform tensile test sample into a composite material at microscopic level. It contains grains and voids in the metal matrix. Strain energy make void wider as tensile loading employed high stress in to the specimen than the fracture toughness. Though, the process of volumetric change in voids and its population transform FSW sample response through degradation in elongation.

Conclusion

In this investigation, the effect of assisted source on to fracture mechanism was analyzed to improve the friction stir welded Cu to SS joint. From this study, the following important conclusion are obtained

a. Most of the sample fractured from WN, some of them fractured from SS TMAZ/ interface and from the SS dispersed particle. It reported lower value of TS

b. Highest joint efficiency (76%) reported when material welded with conventional FSW

c. Additional heating definitely improve the deformation criteria, but location of the torch should be optimized and shifted towards material having higher melting point

d. Pilot hole decreases the load on to the FSW tool while plunge phase, eventually increases the reliability of the tool

e. Tensile fracture has been initiated from the root and it propagated towards the top side reflect the lower density of composite metal matrix of Cu and SS

f. Maximum hardness corresponds to WN which indicate high degree of deformation and continuous dynamic recrystallization

g. Finer grain structure can be obtained by FSW process

h. Larger mixing between the SS Cu materials observed in the weld nugget for FSW specimen welded with additional heating compare to additional cooling indicating poor material flow.

i. Heterogeneous deformation behavior of material land up with localized brittleness within the joint decreases the TS value of WN compare to BM

j. Ductile fracture seen in the case of additional heating whereas brittle fracture when material welded with additional cooling

k. Small, uniformly dispersed SS particle further improve the TS value. This can be achieved by enabling higher degree of deformation of SS

Acknowledgement

The authors are grateful to Pandit Deendayal Petroleum University, Gandhinagar and Board for Research in Fusion Science and Technology (BRFST), Institute for Plasma Research (IPR), Gandhinagar for sponsoring the research project via project number NFP/MAT/A10/04.

References

1. Barabash V, Peacock A, Fabritsiev S, Kalinin G, Zinkle S, et al. (2007) Materials challenges for ITER - Current status and future activities. J Nucl Mater 367-370: 21-32.

2. Federici G, Kemp R, Ward D, Bachmann C, Franke T, et al. (2014) Overview of EU DEMO design and R&D activities. Fusion Eng Des 89: 882-889.

3. Zhang Y, Huang J, Chi H, Cheng N, Cheng Z, et al. (2015) Study on welding-brazing of copper and stainless steel using tungsten/metal gas suspended arc welding. Mater Lett 156: 7-9.

4. Zhang BG, Zhao J, Li XP, Chen GQ (2015) Effects of filler wire on residual stress in electron beam welded QCr0.8 copper alloy to 304 stainless steel joints. Appl Therm Eng 80: 261-268.

5. Roy C, Pavanan VV, Vishnu G, Hari PR, Arivarasu M, et al. (2014) Characterization of metallurgical and mechanical properties of commercially pure copper and AISI 304 dissimilar weldments. Procedia Mater Sci 5: 2503-2512.

6. Roy RK, Singh S, Gunjan MK, Panda AK, Mitra A (2011) Joining of 304SS and pure copper by rapidly solidified Cu-based braze alloy. Fusion Eng Des 86: 452-455.

7. Zapata A (2014) System and method of welding stainless steel to copper.

8. Andreevskikh LA, Drozdov AA, Mikhailov AL, Samarokov YM, Skachkov OA, et al. (2015) Producing bimetallic steel-copper composites by explosive welding. Steel Transl 45: 84-87.

9. Banetta S, Bellin B, Lorenzetto P, Zacchia F, Boireau B, et al. (2015) Manufacturing and testing of a ITER first wall semi-prototype for EUDA pre-qualification. Fusion Eng Des 98-99: 1211-1215.

10. Sahul M, Sahul M, Turňa M, Zacková P (2014) Disk laser welding of copper to stainless steel. Adv Mater Res 1077: 76-81.

11. Kumar N, Yuan W, Mishra RS (2015) Friction stir welding of dissimilar alloys and materials. Elsevier, Netherlands.

12. DebRoy T, Bhadeshia HKDH (2010) Friction stir welding of dissimilar alloys-A perspective. Sci Technol Weld Join 15: 266-270.

13. Thomas WMW, Norris I, Nicholas ED, Watts ER (1991) Friction stir welding-process developments and variant techniques. SME Summit pp. 1-21.

14. Al Jarrah JA, Swalha S, Mansour TA, Ibrahim M, Al Rashdan M, et al (2014) Welding equality and mechanical properties of aluminum alloys joints prepared by friction stir welding. Mater Des 56: 929-936.

15. Thomas WM, Johnson KI, Wiesner CS (2003) Friction stir welding-recent developments in tool and process technologies. Adv Eng Mater 5: 485-490.

16. Zhang DF, Long F, Chen XW, Wen XQ, Luo HS(2011) Review on research status of friction stir welding technology. Adv Mater Res 335-336: 379-382.

17. Mishra RS, Ma ZY (2005) Friction stir welding and processing. Mater Sci Eng R Reports 50: 1-78.

18. Chen CM, Kovacevic R (2004) Joining of Al 6061 alloy to AISI 1018 steel by combined effects of fusion and solid state welding. Int J Mach Tools Manuf 44: 1205-1214.

19. Elrefaey A, Gouda M, Takahashi M, Ikeuchi K (2005) Characterization of aluminum/steel lap joint by friction stir welding. J Mater Eng Perform 14: 10-17.

20. Lee WB, Schmuecker M, Mercardo UA, Biallas G, Jung SB (2006) Interfacial reaction in steel-aluminum joints made by friction stir welding. Scr Mater 55: 355-358.

21. Watanabe T, Takayama H, Yanagisawa A (2006) Joining of aluminum alloy to steel by friction stir welding. J Mater Process Technol 178: 342-349.

22. Uzun H, Dalle Donne C, Argagnotto A, Ghidini T, Gambaro C (2005) Friction stir welding of dissimilar Al 6013-T4 To X5CrNi18-10 stainless steel. Mater Des 26: 41-46.

23. Imani Y, Besharati Givi MK, Guillot M (2011) Improving friction stir welding between copper and 304L stainless steel. Adv Mater Res 409: 263-268.

24. Ramirez AJ, Benati DM (2011) Effect of tool offset on dissimilar Cu-AISI 316 stainless steel friction stir welding. In: Proc. 21st Int. Offshore Polar Eng. Conf. International Society of Offshore and Polar Engineers, Maui, Hawaii, USA. pp. 548-551.

25. Cui S, Chen ZW (2009) Effects of tool speeds and corresponding torque/energy on stir zone formation during friction stir welding/processing. IOP Conf Ser Mater Sci Eng 4: 012019.

26. Kou S (2006) Arc-enhanced friction stir welding.

27. Colligan K (2003) Friction stir welding with simultaneous cooling.

28. Li HB, Jiang ZH, Feng H, Zhang SC, Li L, et al. (2015) Microstructure, mechanical and corrosion properties of friction stir welded high nitrogen nickel-free austenitic stainless steel. Mater Des 84: 291-299.

29. Meran C, Canyurt OE (2010) Friction stir welding of austenitic stainless steels. J Achiev Mater Manuf Eng 43: 432-439.

30. Kumar A, Kumar P, Sidhu BS (2014) Influence of tool shoulder diameter on mechanical properties of friction stir welded dissimilar aluminium alloys 2014 and 6082. 4: 5-10.

31. Sun X (2010) Failure mechanisms of advanced welding processes. Woodhead Publishing Limited, Great Abington, Cambridge, UK.